

Isolation and characterization of impurities in docetaxel[☆]

R. Vasu Dev^a, J. Moses Babu^{a,*}, K. Vyas^a, P. Sai Ram^b, P. Ramachandra^b,
N.M. Sekhar^b, D.N. Mohan Reddy^b, N. Srinivasa Rao^b

^a *Department of Analytical Research, Discovery Research, Dr. Reddy's Laboratories Ltd., Bollaram Road, Miyapur, Hyderabad 500049, Andhra Pradesh, India*

^b *Oncology Operations, Dr. Reddy's Laboratories Ltd., Hyderabad, Andhra Pradesh, India*

Received 17 May 2005; received in revised form 20 October 2005; accepted 21 October 2005

Available online 5 December 2005

Abstract

During the process development of docetaxel, two polar impurities (Impurities I and II) and two non-polar impurities (Impurities III and IV) were detected by high performance liquid chromatography (HPLC). All the impurities were isolated by Medium Pressure Liquid Chromatography (MPLC). The Impurities I, II, III and IV were identified as 13-[(4*S*,5*R*)-2-oxo-4-phenyl-oxazolidine-5-carboxy]-10-deacetyl baccatin III ester, 2'-epi docetaxel, 7-epi docetaxel and 13-[(4*S*,5*R*)-2-oxo-4-phenyl-oxazolidine-3,5-dicarboxyl-3-tert-butyl]-10-deacetyl baccatin III ester, respectively, based on one- (1D) and two-dimensional (2D) nuclear magnetic resonance (NMR) spectroscopy data. The Impurity IV was crystallized and the structure was solved by single crystal X-ray diffraction (XRD). Two impurities (Impurities II and III) were found to be process related, while the remaining two impurities (Impurities I and IV) turned out to be isomers. The formation of these impurities was discussed.

© 2005 Elsevier B.V. All rights reserved.

Keywords: Docetaxel; Impurity; Spectroscopy; Identification; Liquid chromatography-mass spectrometry; MPLC; Characterization

1. Introduction

Docetaxel (trademarked as Taxotere by Rhone-Poulenc Rorer) was approved by the FDA for the treatment of advanced ovarian cancer in April 1994 and in December 1999 for the treatment of patients with locally advanced or metastatic non-small cell lung cancer. Docetaxel (*N*-debenzoyl-*N*-tert-butoxycarbonyl-10-deacetyl taxol) was synthesized in 1985. Docetaxel is obtained by semisynthesis from 10-deacetylbaccatin III, non-cytotoxic precursor extracted from the needles of the European yew, *Taxus baccata* [1]. Taxotere is approximately twice as potent as taxol in inhibiting cold and calcium-induced depolymerization of microtubules [2].

The present study describes the identification of four impurities in crude docetaxel drug [3]. The epimerization of taxane related compounds (e.g., Taxol) is known [4,5]. All the impurities were isolated using MPLC and characterized by using NMR

and mass spectral data. The Impurities I and IV, with oxazolidinone moiety in the side chain appear to be novel and previously unreported.

2. Experimental

2.1. Chemicals

Ammonium acetate (AR grade, SD fine chemicals, India) and acetonitrile (HPLC grade, Merck, India) were purchased. High pure Milli Q water was used with the help of Millipore Milli-Q plus purification system. Crude docetaxel drug sample was analyzed and taken up for this study.

2.2. High performance liquid chromatography (analytical)

A Varian Model ProStar separation module equipped with a Varian ProStar UV detector was used. The HPLC method developed for the analysis of docetaxel and its impurities uses a C18 column (BDS Hypersil C18, 250 mm × 4.6 mm i.d., 5 μm particle size, Thermo Hypersil-Keystone, Germany) with a 60:40 (v/v) mobile phase consisting of 0.02 M ammonium acetate, pH

[☆] Publication No. 330-A.

* Corresponding author. Tel.: +91 40 23045439x258; fax: +91 40 23045438.
E-mail address: mosesbabuj@drreddys.com (J. Moses Babu).

4.5 (adjusted by using acetic acid) and acetonitrile. Detection was carried out at 230 nm and the flow rate was 1.0 ml/min. Data were recorded using Star chromatography workstation Version 5.51 software.

The docetaxel sample was prepared at a concentration of 1 mg/ml in mobile phase for the analytical HPLC.

2.3. Isolation of impurities by MPLC

The crude docetaxel was dissolved in dichloromethane (DCM) and adsorbed over silicagel (mesh 230–400). This adsorbed compound was applied to MPLC (Buchi R688, column: 70 cm × 460 cm, Fraction Collector Buchi 684) using silicagel (mesh 230–400) as adsorbent and eluted with DCM—methanol (MeOH). The elution solvents were classified as (A) dichloromethane and (B) methanol. The impurities were eluted according to the gradient by changing the % of (B) at different times, T (min)/%B = 0/0, 15/0.5, 20/1.0, 30, 1.5, 45/2.0, 90/2.5. Flow rate was 50 ml/min. Fractions of 100 ml were collected, and those exhibiting similar TLC profiles combined. The enriched and purified samples of individual impurities were provided by Oncology Operations, Dr. Reddy's Laboratories Ltd. (DRL).

2.4. Mass spectrometry

Electrospray ionization and tandem mass spectrometry experiments were performed using a triple quadrupole mass spectrometer (PE Sciex model API 3000). The positive and negative electrospray data were obtained by switching the capillary voltage between +5000 and −4500 V, respectively. Collision potential (30 V) and nitrogen gas was used in the collision cell for MS–MS studies.

2.5. NMR spectroscopy

The NMR experiments were performed on Varian spectrometers operating at 400 and 500 MHz in CDCl_3 at 30 °C. The ^1H chemical shift values were reported on the δ scale in ppm, relative to TMS ($\delta=0.00$) and the ^{13}C chemical shift values were reported relative to CDCl_3 ($\delta=77.00$ ppm) as internal standards. Standard pulse sequences provided by Varian were used for distortionless enhancement by polarization transfer (DEPT), gradient double quantum filtered correlation spectroscopy (gDQCOSY), gradient hetero nuclear single quantum coherence spectroscopy (gHSQC), gradient heteronuclear multibond coherence spectroscopy (gHMBC) ($J=8.0$ Hz) experiments. Nuclear overhauser effect spectroscopy (NOESY) experiment was run using a mixing time of 600 ms.

3. Results and discussion

The HPLC chromatogram of crude docetaxel is shown in Fig. 1. The LC/MS data gave the molecular ions of the impurities. The HPLC retention times (RT) and the tentative structures deduced from the MS data are shown in Table 1. The impurities were isolated using MPLC and characterized by NMR and FTIR spectroscopy. The structures of Impurities I, III and IV were confirmed by the spectral data. The NMR data were compared with those of docetaxel (Table 2). Those and other details of the structure elucidation are discussed in the following section.

3.1. Structure Elucidation of Impurity I

The amount of Impurity I increases with time when docetaxel is stored in mobile phase (mobile phase pH is 4.5), which is a qualitative observation. Concomitantly the amount of Impurity

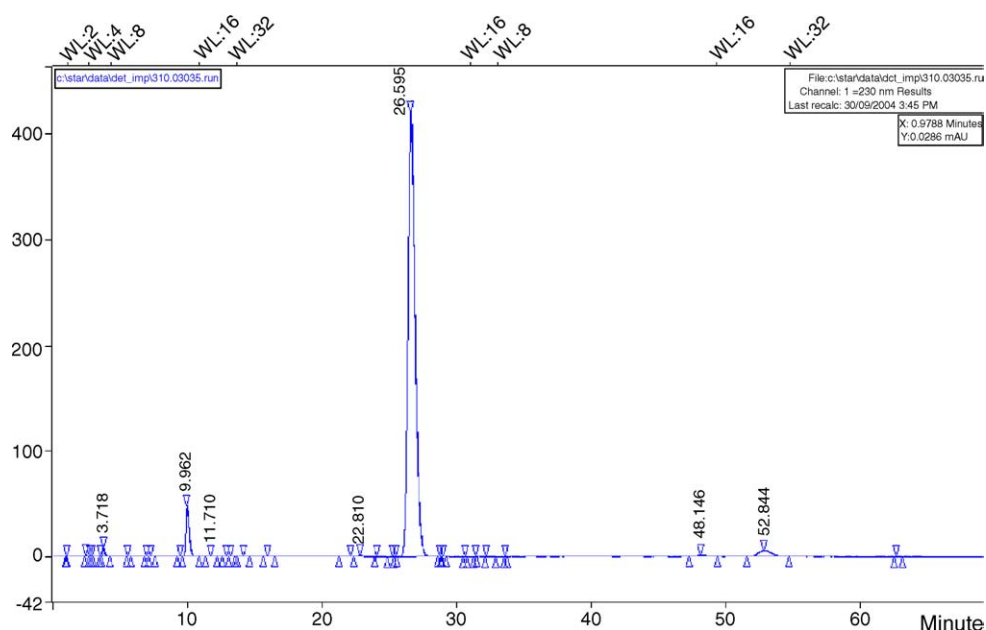


Fig. 1. Docetaxel HPLC chromatogram. Column: Hypersil BDS C18, 250 mm × 4.6 mm, mobile phase: 0.02 M $\text{CH}_3\text{COONH}_4$, pH 4.5 (adjusted by using acetic acid) in water:acetonitrile (60:40), flow rate = 1.0 ml/min, wavelength at UV 230 nm.

IV decreases, indicating either that Impurity IV converts to Impurity I. The electrospray ionization (ESI) mass spectrum of Impurity I showed a molecular ion at m/z 733, indicating that Impurity I has a molecular mass less than that of docetaxel (74 Da). The ^1H NMR spectrum showed the absence of methyl signals for the tertiary butyl group and, 2'-hydroxyl group protons. The 4'-NH proton signal appears at 6.64 ppm, which appears at 5.42 ppm in docetaxel. The proton data is supported by the ^{13}C NMR spectrum in which the signals due to C5', C6', C7', C8' and C9' were found to be absent. All of these data would indicate the absence of *t*-butyloxy group. Furthermore, there was a new ^{13}C signal at 157.64 ppm, which exhibited

gHMBC correlations with methine protons at C2', C3' and the exchangeable proton at 6.64 ppm. Taken together, these observations are consistent with the formation of the oxazolidinone ring in Impurity I. In the FTIR spectrum of Impurity I, the intensity of the bands in the range 3400–3600 cm^{-1} was less than for those observed for docetaxel. This behavior indicates the change in either or both the OH and NH groups in Impurity I. Furthermore, the FTIR spectrum of Impurity I was found to be well resolved in the range 1600–1800 cm^{-1} . This is indicative of a change in carbonyl functional groups or environment. The observations from the FTIR spectra match well with those from NMR data. Based on this spectral data, the

Table 1
Retention time, molecular weight and atom numbering of the impurities

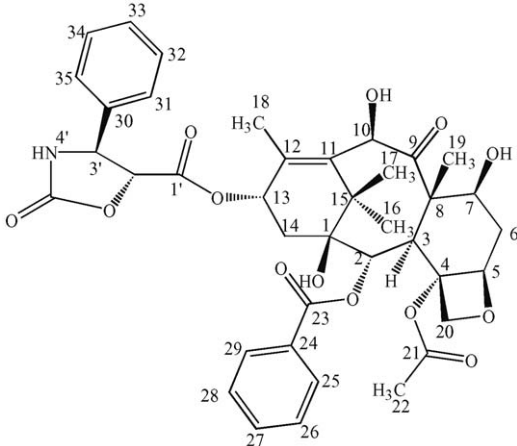
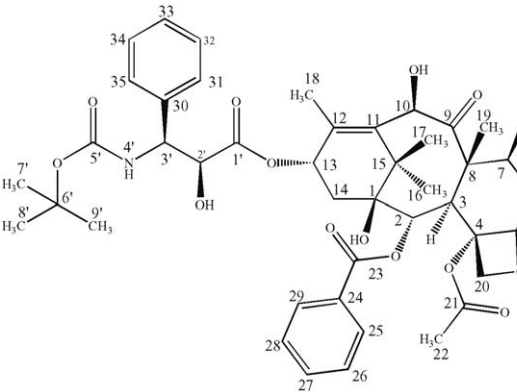
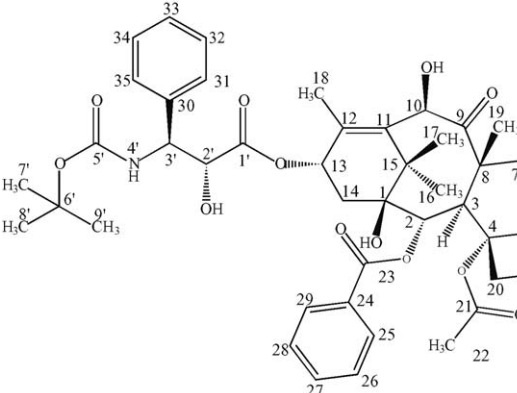
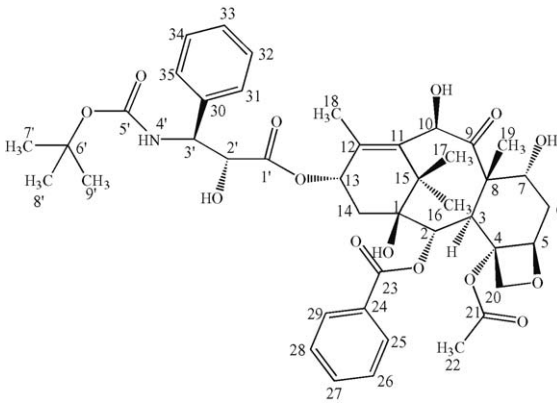
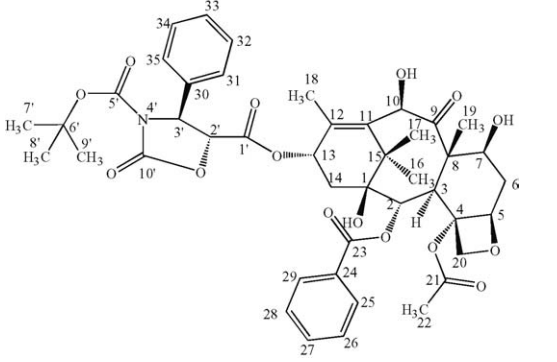
No.	RT (HPLC) (min)	Structure	m/z	Area %
Impurity I	9.96		733	4.54
Impurity II	22.81		807	0.26
Docetaxel	26.60		807	91.91, API

Table 1 (Continued)

No.	RT (HPLC) (min)	Structure	<i>m/z</i>	Area %
Impurity III	48.15		807	0.43
Impurity IV	52.84		833	2.30

Impurity I was characterized as 13-[(4*S*,5*R*)-2-oxo-4-phenyl-oxazolidine-5-carboxy]-10-deacetyl baccatin III ester.

3.2. Structure elucidation of Impurity II

The ESI mass spectrum of Impurity II gave a protonated molecular ion at *m/z* 808, which is the same as docetaxel. This indicates that Impurity II could be an isomer of docetaxel. Also, there was no significant difference was observed, on comparison of between the NMR data of Impurity II with and docetaxel (Table 2). But for a small but significant difference in the retention time in HPLC data, all the spectral data match reasonably well with those of docetaxel. As there is no difference in the NMR data pertaining to baccatin III ring, it is reasonable to conclude that Impurity II could be a diastereoisomer arising due to a change in stereochemistry in the side chain of the docetaxel, i.e. at C2' and/or C3'. The stereochemistry docetaxel is 2'*R*, 3'*S*. Hence the possible structures of Impurity II could be one of the three isomers viz (2'*S*, 3'*S*), (2'*S*, 3'*R*) and (2'*R*, 3'*R*). But the tentative structure expected from the process is 2'-epi docetaxel.

The NOESY data did not show any difference in the correlations when compared with those observed in docetaxel.

3.3. Structure elucidation of Impurity III

The ESI positive ion mass spectrum of Impurity III gave a protonated ion at *m/z* 808, which is same as docetaxel. This

indicates that Impurity III could also be an isomer of docetaxel. The ¹H NMR spectrum of Impurity III showed a significant change in the ¹H chemical shifts of the protons at C6, and C7 and the hydroxyl proton of C7. The same trend is observed with the ¹³C chemical shifts of C5, C6 and C7, which would be consistent with a change in the stereochemistry at C7 position.

The NOESY correlations in Impurity III were compared with those of docetaxel. In docetaxel the methine proton at C7 (4.24 ppm) showed through space correlation with protons at C10 (5.20 ppm), C3 (3.91 ppm) and C6 (2.59 ppm). On the other hand, in the Impurity III, the methine proton at C7 (3.67 ppm) showed correlation with protons at C10 (5.45 ppm), C7–OH (4.70 ppm) and C6 (2.35 ppm) and C19 (1.72 ppm). The following observation is noteworthy. The correlation of the proton at C7 with the protons at C3 (3.93 ppm) is not observed in Impurity III, while a new correlation is seen with protons at C19 (1.72 ppm). These through-space correlations from NOESY data clearly indicate that the proton at C3 is situated farther from the proton at C7, while being closer to the protons at C19. Since the methyl group at C19 is in β configuration, it follows that the methine proton at C7 also is also in β configuration. Hence, the structure of Impurity III is assigned to be 7-epi isomer of docetaxel (NOESY interactions are shown by arrows in Fig. 2). Based on all of the spectral data, the Impurity III was characterized as 7-epi docetaxel.

Table 2
¹H and ¹³C NMR data of docetaxel, Impurities I, IV, II and III

Position ^a	¹ H	Docetaxel		Impurity I		Impurity IV		Impurity II		Impurity III	
		δ (ppm) (Hz) ^b	¹³ C	δ (ppm) (Hz)	¹³ C	δ (ppm) (Hz)	¹³ C	δ (ppm) (Hz)	¹³ C	δ (ppm) (Hz)	¹³ C
1	–	–	78.80	–	79.19	–	79.13	–	78.90	–	79.23
2	1H	5.68 (d, 7.0)	74.80	5.66 (d, 7.5)	75.03	5.69 (d, 7.0)	74.92	5.68 (d, 7.0)	74.76	5.74 (d, 7.0)	75.44
3	1H	3.91 (d, 7.0)	46.46	3.91 (d, 7.5)	46.24	3.94 (d, 7.0)	46.38	3.96 (d, 7.0)	46.64	3.93 (d, 7.0)	40.29
4	–	–	81.07	–	80.48	–	80.23	–	81.13	–	82.11
5	1H	4.95 (dd, 10.0, 2.0)	84.11	4.92 (dd, 8.8, 1.5)	84.47	4.93 (dd, 2.0, 9.5)	84.85	4.96 (d, 8.0)	84.17	4.90 (dd, 4.0, 9.5)	82.63
6	Ha	2.59 (ddd, 7.0, 10.0, 16.5)	37.01	2.55 (m)	36.60	2.60 (ddd, 6.5, 9.5, 14.0)	36.82	2.62 (ddd, 4.5, 9.5, 15.0)	37.00	2.35 (m)	35.35
	Hb	1.85 (m)	–	1.88 (m)	–	1.85 (ddd, 2.0, 14.0, 14.0)	–	1.87 (dt, 2.5, 15.0)	–	–	–
7	1H	4.24 (m)	72.00	4.30 (m)	71.47	4.27 (br, m)	71.79	4.26 (m)	71.98	3.67 (dd, 2.5, 10.0)	75.86
	OH	1.50 (br)	–	2.92 (d, 6.0)	–	1.51 (br, s)	–	1.52 (d, 8.5)	–	4.70 (d, 10.0)	–
8	–	–	57.64	–	57.89	–	57.53	–	57.69	–	57.31
9	–	–	211.34	–	210.91	–	211.12	–	211.31	–	215.04
10	1H	5.20 (d, 1.5)	74.53	5.35 (s)	74.16	5.22 (s)	74.30	5.25 (d, 1.5)	74.56	5.45 (s)	77.90
	OH	4.20 (d, 1.5)	–	4.88 (s)	–	4.21 (s)	–	4.22 (d, 1.5)	–	4.12 (s)	–
11	–	–	135.95	–	136.25	–	137.62	–	135.81	–	135.60
12	–	–	138.42	–	138.17	–	138.20	–	138.60	–	138.11
13	1H	6.22 (t, 8.5)	72.43	6.33 (t, 9.0)	72.30	6.3 (t, 9.0)	72.91	6.17 (br)	72.47	6.26 (br)	72.35
14	2H/Ha	2.27 (d, 8.5)	35.72	2.26 (d, 9.0)	35.81	Ha 2.30 (dd, 9.0, 15.0)	35.84	2.38 (dd, 9.0, 15.0)	36.23	2.33 (m)	36.18
	Hb	–	–	–	–	Hb 2.22 (dd, 9.0, 15.0)	–	2.17 (dd, 9.0, 15.0)	–	–	–
15	–	–	43.07	–	43.13	–	43.10	–	42.94	–	42.57
16	3H	1.24 (s)	26.44	1.22 (s)	26.53	1.26 (s)	26.53	1.22 (s)	26.47	1.24 (s)	25.95
17	3H	1.14 (s)	20.62	1.11 (s)	20.81	1.14 (s)	20.71	1.14 (s)	20.30	1.10 (s)	20.57
18	3H	1.85 (s)	14.36	2.0 (s)	14.17	1.98 (s)	14.33	2.01 (d, 1.5)	14.67	1.80 (s)	14.45
19	3H	1.76 (s)	9.84	1.73 (s)	9.96	1.75 (s)	9.90	1.77 (s)	9.83	1.72 (s)	16.66
20	Ha	4.31 (d, 8.5)	77.30	4.28 (d, 8.5)	76.40	4.30 (d, 8.5)	76.45	4.32 (d, 8.5)	77.20	4.38 (d, 10.0)	77.75
	Hb	4.20 (d, 8.5)	–	4.15 (d, 8.5)	–	4.15 (d, 8.5)	–	4.18 (d, 8.5)	–	4.37 (d, 10.0)	–
21	–	–	170.29	–	170.25	–	169.88	–	169.59	–	172.27
22	3H	2.37 (s)	22.55	2.23 (s)	21.83	2.15 (s)	21.76	2.22 (s)	22.58	2.48 (s)	22.52
23	–	–	167.02	–	167.05	–	167.01	–	166.96	–	167.12
24	–	–	128.82	–	129.36	–	128.65	–	129.18	–	129.33
25 and 29	2H	8.10 (d, 7.5)	130.16	8.05 (d, 7.5)	130.06	8.06 (dd, 1.0, 8.0)	130.03	8.05 (dd, 1.0, 8.0)	130.20	8.13 (d, 8.0)	130.18
26 and 28	2H	7.50 (t, 7.5)	128.70	7.47 (t, 7.5)	128.66	7.48 (dt, 2.0, 8.0)	128.65	7.47 (t, 7.5)	128.68	7.51 (t, 8.0)	128.76
27	1H	7.61 (t, 7.5)	133.70	7.61 (t, 7.5)	133.78	7.62 (dt, 1.5, 8.0)	133.79	7.61 (dt, 1.0, 8.0)	133.76	7.62 (t, 8.0)	133.66
30	–	–	138.42	–	138.64	–	137.62	–	138.60	–	138.45
31 and 35	2H	7.36–7.42 (m)	128.82	7.30–7.50 (m)	129.49	7.42–7.50	129.39	7.47 (t, 7.5)	128.85	7.41 (m)	126.62
34 and 32	2H	7.36–7.42 (m)	126.75	7.30–7.50 (m)	125.86	7.36 (m)	125.80	7.40 (t, 7.5)	127.09	7.38 (m)	128.86
33	1H	7.32 (m)	129.15	7.30–7.50 (m)	129.17	7.42–7.50	129.13	7.33 (dt, 1.5, 7.0)	128.15	7.32 (t, 7.0)	128.03
1'	–	–	172.63	–	168.85	–	167.89	–	172.55	–	172.67
2'	1H	4.62 (br, s)	73.68	4.83 (d, 5.0)	80.66	4.74 (d, 4.0)	76.88	4.48 (br, s)	73.90	4.63 (br, s)	73.72
	OH	3.35 (d, 5.0)	–	–	–	–	–	3.41 (br)	–	3.31 (br, s)	–
3'	1H	5.26 (d, 8.5)	56.23	5.10 (d, 5.0)	59.66	5.37 (d, 4.0)	61.92	5.23 (br)	56.44	5.28 (br)	56.60
4'	1H	5.42 (d, 8.5)	–	6.64 (s)	–	–	–	5.37 (d, 8.5)	–	5.42 (d, 9.5)	–
5'	–	–	155.32	–	–	–	148.01	–	155.20	–	155.36
6'	–	–	80.23	–	–	–	84.28	–	80.31	–	80.20
7', 8', 9'	9H	1.35 (s)	28.19	–	–	1.35 (s)	27.64	1.39 (s)	28.23	1.32 (s)	28.16
10'	–	–	–	–	157.64	–	150.31	–	–	–	–

s, singlet; d, doublet; dd, doublet of doublet; ddd, doublet of doublet of a doublet; t, triplet; m, multiplet; br, broad.

^a Refer the structural formula given above for numbering.

^b This column gives the chemical shift, multiplicity and coupling constant.

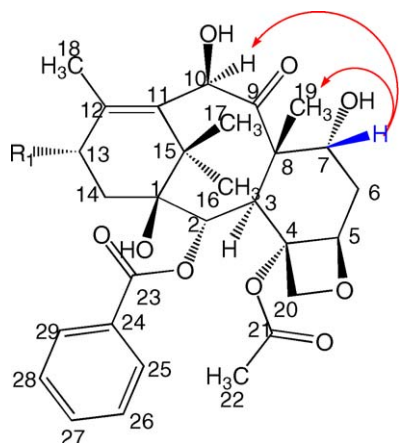


Fig. 2. Important NOESY interaction observed in Impurity III.

3.4. Structure elucidation of Impurity IV

The ESI mass spectrum showed a molecular ion at m/z 833, 26 mass units higher than that of Impurity IV. The mass spectrum of docetaxel gave a fragment ion at m/z 527, which would correspond to removal of the side chain. Interestingly, Impurity IV also displayed the same fragment at m/z 527. Thus, comparison of the fragmentation pattern of Impurity IV and docetaxel indicates that these two compounds differ from each other in the presence or absence of the side chain.

The NMR spectroscopy data (both ^1H and ^{13}C) for Impurity IV were compared with the respective data of docetaxel (Table 2). The ^1H chemical shifts of the methine protons at C2' and C3' were deshielded in Impurity IV, when compared to docetaxel. Furthermore, the signals due to the exchangeable protons at 4'-NH and 2'-OH were not observed. The chemical shifts of the remaining ^1H signals were comparable. The ^{13}C chemical shifts of the carbons, C1', C2', C3', C5' and C6'

showed significant difference. Moreover, an additional signal at 150.31 ppm was observed, which could be attributed to a carbonyl functionality.

In the FTIR spectrum of Impurity IV, the intensity of the bands in the range 3400–3600 cm^{-1} was less intense when compared to docetaxel. This indicates that some change has occurred in either the OH or NH groups of Impurity IV. Furthermore, the FTIR spectrum of Impurity IV was found to be well resolved in the range 1600–1800 cm^{-1} when compared to docetaxel, indicating a change in the carbonyl functional groups or their environment. The observations from the FTIR spectra match well with those from NMR data. The extra 26 mass units observed for Impurity IV can be rationalized in terms of the incorporation of a carbonyl group and the removal of two hydrogen atoms. In the gHMBC experiment of Impurity IV, the additional quaternary ^{13}C signal at 150.31 ppm was found to show through bond [^1H - ^{13}C] correlations with the methine protons at C2' (4.74 ppm) and C3' (5.37 ppm) (Fig. 3). These correlations clearly indicate formation of an oxazolidinone ring by the incorporation of a carbonyl group and elimination of the exchangeable protons at 4'-NH and 2'-OH. Based on the spectral data, the Impurity IV was assigned as 13-[(4*S*,5*R*)-2-oxo-4-phenyl-oxazolidine-3,5-dicarboxyl-3-tert-butyl]-10-deacetyl baccatin III ester.

The structure was unambiguously confirmed by a single crystal XRD experiment. Single crystals suitable for XRD studies were grown from a solution of ethanol and acetonitrile. The ORTEP diagram of Impurity IV crystal structure is shown in Fig. 4 and the crystal data are shown in Table 3. The baccatin III ring is puckered in such a way that it takes a shape resembling the letter U. The five-membered oxazolidinone ring assumes a half chair conformation where the atoms C2' and C3' are displaced from the plane defined by the atoms C10', N4' and O2'. The six membered ring consisting of the atoms C1, C15, C11, C12, C13 and C14 assumes boat conformation where the atoms C13 and C15 are displaced in the same direction from the plane defined by

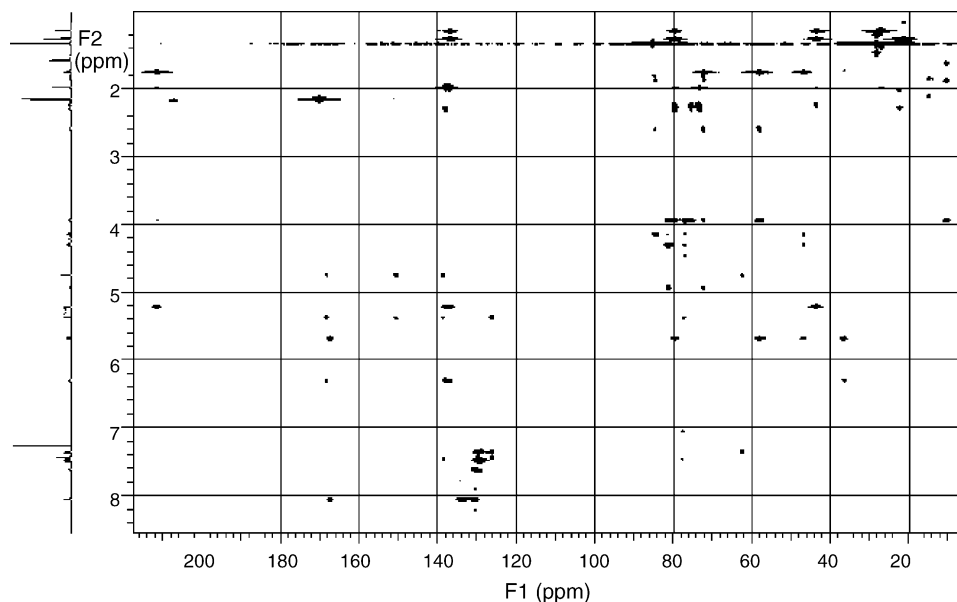


Fig. 3. gHMBC NMR spectrum (500 MHz) of Impurity IV.

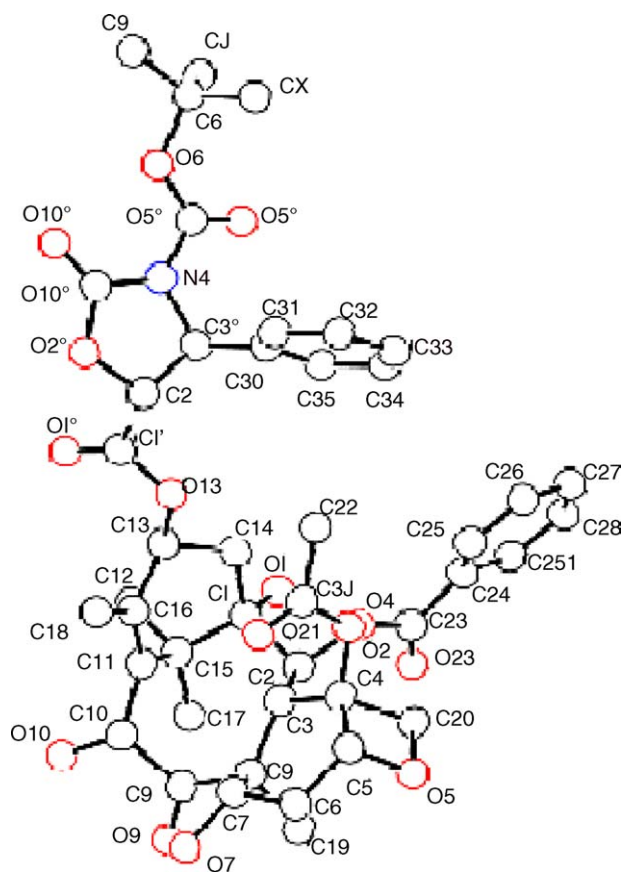


Fig. 4. Molecular structure of Impurity IV.

the rest of the atoms. On the other hand, the six membered ring consisting of the atoms C3, C4, C5, C6, C7 and C8 assumes a half chair conformation wherein the atoms C7 and C8 displaced in opposite directions from the plane defined by the rest of the atoms. The intramolecular interactions, such as O–H···O and C–H···O (Table 4) influence the observed conformation of the molecule.

In the lattice, the molecules are connected together by intermolecular O–H···O hydrogen bonding interactions (Table 4).

Table 3
Crystal data

Parameters	Details
Name of the molecule	Impurity IV
Empirical formula	C ₄₄ H ₅₁ NO ₁₅
Molecular weight	833.88
Crystal system	Monoclinic
Space group	P2 ₁ (#4)
Lattice type	Primitive
Cell parameters	
<i>a</i> (Å)	13.284(4)
<i>b</i> (Å)	12.726(4)
<i>c</i> (Å)	13.545(4)
β (°)	115.832(3)
Volume (Å ³)	2060.9(11)
Z-value	2
<i>D</i> _{calc} (g cm ⁻³)	1.344

Table 4
Geometrical parameters of intramolecular interactions

D	H	A	D–H	H···A	D···A	D–H···A	^a Symm(A)
O10	H47	O9	1.01(6)	1.85(6)	2.641(7)	132(5)	I
C17	H8	O9	0.950(11)	2.459(9)	3.088(9)	123.6(7)	I
C16	H10	O1	0.949(12)	2.494(10)	2.857(10)	102.7(7)	I
C8'	H17	O5'	0.95(2)	2.469(19)	3.081(18)	122.1(16)	I
C7'	H22	O5'	0.951(17)	2.348(13)	2.992(13)	124.6(13)	I
C18	H27	O13	0.950(13)	2.286(10)	2.801(10)	113.3(8)	I
C14	H29	O2	0.950(9)	2.404(7)	2.813(7)	105.7(6)	I
C19	H36	O5	0.951(13)	2.481(12)	3.320(12)	147.3(8)	I
C3	H41	O21	0.951(8)	2.592(10)	3.142(9)	117.2(6)	I
C2	H45	O23	0.950(9)	2.360(7)	2.744(7)	103.6(6)	I
O10	H47	O1'	1.01(6)	2.37(7)	3.036(9)	123(5)	II
O7	H48	O10	0.73(5)	2.36(5)	2.962(8)	141(5)	II
C5	H50	O10'	0.950(12)	2.457(9)	3.117(10)	126.5(6)	III
C29	H5	O1'	0.950(12)	2.502(9)	3.159(10)	126.3(7)	IV
C22	H38	O10'	0.950(11)	2.213(9)	3.140(9)	164.9(8)	V
C3'	H42	O23	0.950(10)	2.407(8)	3.335(8)	165.2(7)	VI

^a Symmetry codes of (A); I: *x*, *y*, *z*; II: $-x$, $-1/2+y$, $1-z$; III: *x*, $-1+y$, *z*; IV: $-x$, $-1/2+y$, $-z$; V: $2-x$, $-1/2+y$, $2-z$; VI: $-x$, $1/2+y$, $-x$.

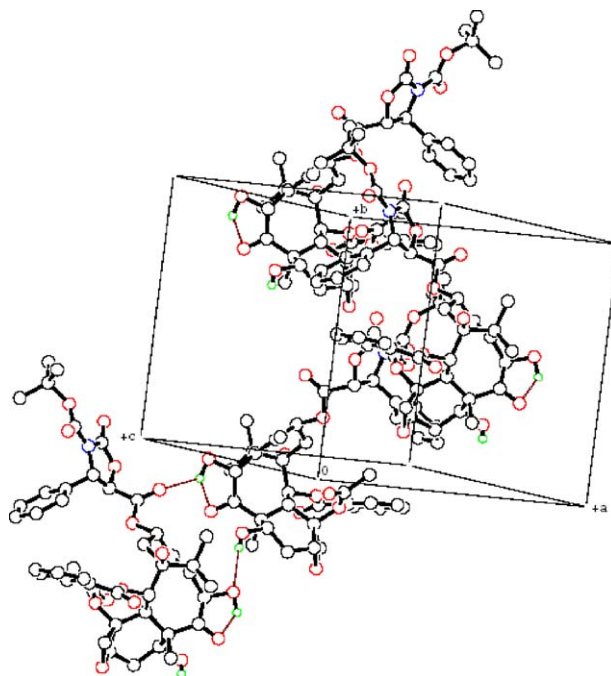
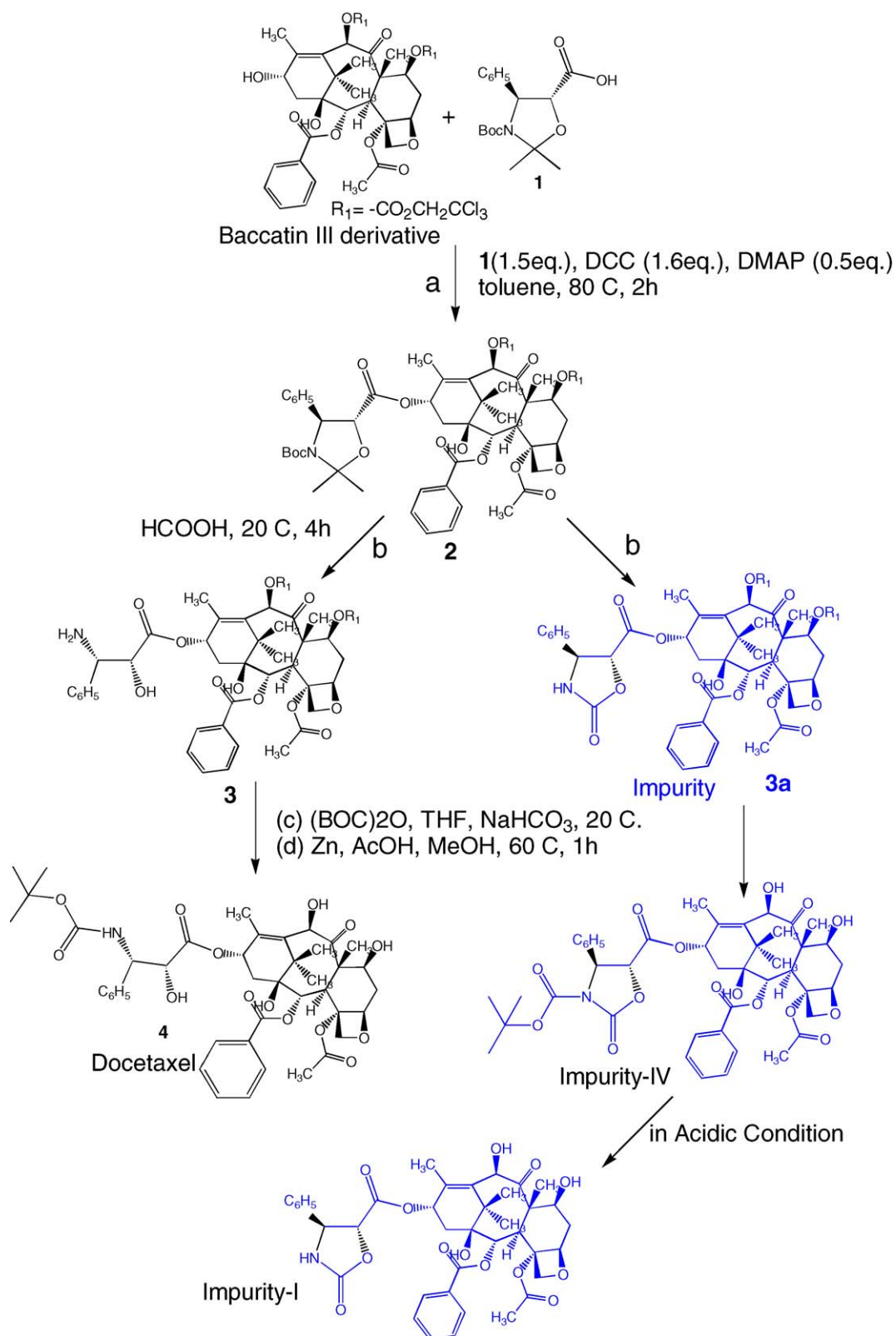


Fig. 5. Packing diagram of Impurity IV.

The stability to the molecules in the lattice comes from C–H···O interaction (Table 4). The packing of the molecules in the lattice showing the hydrogen bonding interactions is depicted in Fig. 5.

4. Formation of impurities

In the presence of formic acid, the derivative of baccatin III, **2**, gives the 'precursor' **3a**, which is subsequently carried through further steps in the synthesis, including the introduction of BOC in the side chain and deprotecting of the hydroxyl groups in baccatin III moiety. These processes lead to the formation of Impurity IV along with docetaxel (shown in Scheme 1). Impurity I forms from Impurity IV under acidic conditions, and Impurities



Scheme 1. Synthesis docetaxel and possible formation of Impurities I and IV.

II and III were formed by the epimerization of 2' and 7 hydroxyl groups [4,5], respectively, and are found to be process related. The synthesis of docetaxel [6] and the formation of impurities are shown in Scheme 1.

Acknowledgements

The authors wish to thank the management of Discovery Research, Dr. Reddy's Laboratories for permitting this work to

be published. The useful discussions with Dr. Selva Kumar are appreciated. Cooperation extended by all the colleagues of Analytical Research division, is gratefully acknowledged.

References

- [1] L.O. Zamir, M.E. Nedeia, S. Belair, F. Sauriol, O. Mamer, E. Jacquemain, F.I. Jean, F.X. Garneau, *Tetrahedron Lett.* 33 (1992) 5173–5177.
- [2] F. Gueritte-Voegelein, D. Guenard, F. Lavelle, M.-T. LeGoff, L. Mangatal, P. Potier, *J. Med. Chem.* 34 (1993) 992–998.
- [3] K.J. Volk, S.E. Hill, E.H. Kerns, M.S. Lee, *J. Chromatogr. B* 696 (1997) 99–115.
- [4] S.-H. Chen, S. Huang, J. Wei, V. Farina, *Tetrahedron* 49 (1993) 2805–2828.
- [5] M. Suffness, *TAXOL: Science and Applications*, CRC Press, 1995.
- [6] A. Commercon, D. Bezar, F. Bernard, J.D. Bourzat, *Tetrahedron Lett.* 33 (1992) 5185–5188.